Multi-scale structural and digestion properties of wheat starches with different amylose contents

Article *in* International Journal of Food Science & Technology · June 2014

DOI: 10.1111/ijfs.12593

5 authors, including:

Zhongkai Zhou
Charles Sturt University
143 PUBLICATIONS **5,005** CITATIONS
SEE PROFILE

Zhiwei Wang
Tianjin University of Science and Technology
17 PUBLICATIONS **211** CITATIONS
SEE PROFILE

International Journal of
Food Science & Technology

International Journal of Food Science and Technology 2014, **49**, 2619–2627

Original article

Multi-scale structural and digestion properties of wheat starches with different amylose contents

Zhongkai Zhou,* Yan Zhang, Xiaoshan Chen, Min Zhang & Zhiwei Wang

Key Laboratory of Food Nutrition and Safety, Ministry of Education, Tianjin University of Science and Technology, Tianjin 300457, China

(Received 17 March 2014; Accepted in revised form 1 May 2014)

Summary The physicochemical and digestion properties of three wheat starches with different amylose contents were studied. Scanning electron microscopy (SEM) showed they displayed a spherical disc-like form, a lenticular shape and an irregular morphology, respectively. Compared with waxy and normal wheat starches, high-amylose wheat starch (HAWS) was characterised by the presence of lower molecular weight amylose fraction, and its granules demonstrated the highest resistance to the cooking. The changes in the IR ratio 1022/999–1047/1022 cm^{-1} following the gel storage suggested the molecules of HAWS are more readily to re-associate and re-organise into a more organised status than other two starches. The determination of glucose release showed that HAWS had the lowest digestion kinetics ($P < 0.001$), and this difference in the digestion properties between HAWS and the other two starches might imply that starch molecular structure, in particular amylose structure is another key factor for manipulating starch digestion property rather than amylose content alone.

Keywords Amylose, digestion, molecular structure, morphology, wheat starch.

Introduction

As a major plant metabolite, starch acts as a major energy source for the diet of most humans (Björck *et al*., 1994). It was well known that the control of glucose releasing rate from starch present in processed foods may play important roles in human health by maintaining a proper blood glucose level and providing extended energy supply (Kumar & Prabhasankar, 2014; Świeca *et al*., 2013). It has been confirmed that the long-term consumption of starchy foods with high glycaemic index (GI) has been highly related to obesity, diabetes and coronary heart disease (Skrabanja *et al*., 1999; Ludwig, 2003). Thus, the digestion property of starch is crucial in a balanced human diet. According to digestion properties, starch can be classified into three groups, rapidly digestible starch (RDS), slowly digestible starch (SDS) and resistant starch (RS) to specify the quality of starch in food products (Englyst *et al*., 1992; Ludwig, 2003). In the three starch groups, SDS is considered beneficial for the host to control glucose release; RS can reach the large bowel to act as a substrate for microbial fermentation to produce a number of active metabolites, for example short-chain fatty acids (SCFA). Meanwhile, RS can also be used as a prebiotics for promoting the growth of probiotics at human gut (Zhou *et al*., 2013). Studies have shown that SCFA is important for maintaining normal colonic function and health (Englyst & Hudson, 1996; Bird *et al*., 2000). Among the various SCFA, butyrate appears to be particularly important in this regard, which is the preferred fuel for colonocytes, plays a role in preserving a normal cellular phenotype, and is involved in the maintenance of an epithelial barrier function and modulation of mucin secretion (Barcelo *et al*., 2000; Topping & Clifton, 2001). Although the susceptibility of starch to hydrolysis by amylases has been shown to be influenced by many factors, for example processing method, food texture and food compositions (Englyst *et al*., 1992; Tovar *et al*., 1992), hydrolysis of starch by amylases is certainly influenced by the physicochemical properties of the starch itself (Slaughter *et al*., 2001; Zhou *et al*., 2010). Our previous study confirmed that molecular structure is considered to be one of the most important factors influencing starch property in terms of digestion (Zhou *et al*., 2010). Thus, in recent years, an increasing number of studies have focused on manipulating starch molecular structure to alter its digestion properties. For instance, clear-cut involvement of branching enzymes of the A family in amylopectin

*Correspondent: Fax: +86 22 60 60 13 71;
e-mail: zkzhou@tust.edu.cn

doi:10.1111/ijfs.12593

synthesis has been demonstrated in rice (Man *et al.*, 2012), barley (Bird *et al.*, 2008) and wheat (Regina *et al.*, 2006). In these cases, the mutants displayed a similar phenotype, that is, a reduction in starch correlated to a large increase in amylose. In maize, this is also accompanied by a switch from the A-type to the B-type of diffraction pattern and by a net loss in crystallinity (Shrestha *et al.*, 2012).

Most of previous studies focused on the effect of amylose content on the starch digestibility (Frei *et al.*, 2003; Chung *et al.*, 2010; Zhu *et al.*, 2011), and these studies used starches with wide ranges of amylose contents (e.g. 1.7% to 55.4% amylose), allowing the correlation between starch digestibility and amylose content to be easily achieved, but not the fine structures. Nevertheless, starch assimilation in the human gastrointestinal tract is a complex process, and the knowledge of the specific molecular properties that are responsible for resistance to enzymatic digestion is still very limited. Based on above considerations, it is necessary to investigate how the morphology, cooking properties and digestion behaviours are influenced by molecular structures of different wheat starches. In this study, three starches isolated from waxy, normal and high-amylose wheat are used. The different resistance to amylase digestion of the three wheat starches is investigated. Moreover, the mechanism on forming more organised structures of starch containing lower molecular weight (MW) amylose fraction will be discussed here.

Materials and methods

Starch materials

Three wheat (*Triticumaestivum* L.) cultivars (normal; lacking starch synthase II polypeptide from A and B genomes and an amylose-free wheat line lacking granule bound starch synthase) from wheat breeding programmes, located at School of Food Engineering and Biotechnology, Tianjin University of Science & Technology, Tianjin, China, were used, and the isolation of starch granules from the wheat flour was performed using the reported method (Finnie *et al.*, 2010). Amylose content of waxy, normal and high-amylose wheat starches (HAWSs) was determined according to the approved method 61-03 (AACC International, 2000) with nil, 26.5 and 78.7%, respectively. Artificial saliva α-amylase (A-3176, Type VI-B from porcine pancreas), amyloglucosidase (A7095, from *Aspergillus niger*) and pepsin (P6887, from porcine gastric mucosa) were purchased from Sigma-Aldrich (St. Louis, MO, USA). Glucose assay kit (GOPOD method) was obtained from Megazyme International Ireland (Wicklow, Bray). Other chemicals were reagent grade and used as received.

Starch cooking

Sixty milligram of starch was mixed with 10 mL of reverse osmosis (RO) water in 25-mL test tubes. The tube was capped and placed in a boiling water bath for 10-min treatment and then quickly cooled to room temperature using tape water. After the collection by centrifugation at 2900 ***g*** for 10 min, the precipitate was washed by 80% EtOH (v/v). The residue was air-dried and used for scanning electron microscopy (SEM) visualisation.

Preparation of precipitated starch

Twenty milligram of starch was added into aqueous dimethylsulphoxide (8 mL, 90:10, DMSO/water, v/v) in a 25-mL test tube. The tube was capped and treated at boiling water bath for 1 h. After cooled by tape water, the mixture was centrifuged at 2095 ***g*** for 10 min, the supernatant was collected into a 25-mL test tube and the dissolved starch was precipitated by adding 18 mL of 95% ethanol. The tube was kept at room temperature overnight and then centrifuged (2095 ***g*** for 15 min). The precipitated starch was collected and then washed twice with 95% ethanol.

One gram of the precipitated starch was mixed with 5 mL RO water and vigorously shaken. The solution was then stored at 4 °C to allow starch molecules to re-associate again, and the changes in IR spectrum were measured using a Fourier transform infra-red spectroscopy (FTIR).

Fourier transform infra-red spectroscopy

A Varian spectrometer (Model: Excalibur 3100; Varian, Inc., Walnut Creek, CA, USA) equipped with a cooled deuterated triglycine sulphate (DTGS) detector was applied for studying FTIR spectrum of the starches. The measurement was taken on a MIRacle™ attenuated total reflectance (ATR) crystal plate with a digital readout high-pressure clamp (Pike Technologies, Madison, WI, USA). The precipitated starch prepared as above was mixed vigorously with 5 mL RO water. After centrifuged at 4 °C, the starch gel was directly loaded on the plate and scanned in the range of 3600–600 cm^{-1} at a resolution of 4 cm^{-1}. Prior to recording, the spectrum was transformed against an empty cell as background. Finally, the spectrum was ATR deconvoluted using a VARIAN RESOLUTIONS PRO software. A half-bandwidth of 15 cm^{-1} and a K factor of 1.5 with triangular apodisation were applied. The IR absorbance values ranging 1200 and 800 cm^{-1} for each starch gel at different storage intervals of 0, 2, 10 and 20 h were obtained via each scanning.

Size-exclusion high-performance liquid chromatography (SE-HPLC)

The precipitated starch (20 mg, wet base) was mixed with 0.5 mL of 0.2 M NaOH and shaken vigorously for 5 s. It was neutralised after the addition of 0.5 mL sodium acetate buffer (0.05 M, pH 4.0) and then 0.20 g ion-exchange resin (BioRad AG 501-X8, Hercules, CA, USA) added and incubated at 50 °C for 1.5 h with occasional shakings. After centrifuged at 10 625 *g* for 10 min, the clear supernatants were collected for SE-HPLC analysis. The HPLC system contains a GBC pump (LC 1150; GBC Instruments, Dandenong, Vic., Australia) equipped with an auto sampler (GBC, LC1610) and an evaporative light scattering detector (ALLTech, Deerfield, IL, USA). The columns are an Ultrahydrogel of 1000 column, an Ultrahydrogel of 250 column and a guard column (7.8 × 300 mm, Waters, Tokyo, Japan) and maintained at 35 °C during HPLC run. Ammonium acetate buffer (0.05 M; pH 5.2) was used as mobile phase at a flow rate of 0.8 mL min^{-1}. Conditions used for the detector are 115 °C for tube temperature and 2.0 L min^{-1} of N_2 gas flow rate.

Starch digestion

Starch was digested using a simulated human small intestinal digestion system following the method described by Htoon *et al.* (2009). Briefly, the starch was pretreated using artificial saliva α-amylase (Sigma A-3176) in carbonate buffer at pH 7.0 and then mixed with pepsin after acidification by HCl. The mixture was neutralised by NaOH and then was digested by pancreatin and amyloglucosidase at physiological pH (6.0) and temperature for incubating 0.0, 1.5, 3.0, 8.0, 12 or 24 h. The supernatant was removed at the end of the chosen incubation time by centrifugation and analysed for glucose content. After the digestion, the indigestible starch (i.e. RS) was collected, freeze-dried and analysed for its physicochemical property. The digestibility for each starch was calculated as the percentage of digested starch in the total starch at the designated incubation intervals. The amount of released glucose from the digested starch was measured using Megazyme glucose assay kit (GOPOD method), and the amount of digested starch was calculated after the conversion of released glucose into starch by use of factor 0.9.

Scanning electron microscopy

The freeze-dried starch and digestion residues prepared as above were sprinkled onto circular aluminium stubs containing double sticky tape. The stubs were then coated with gold using a Hitachi 1B-3 ion coater. The morphology of starch and the digestion residues were visualised by a scanning electron microscope (Autoscan Systems Pty. Ltd., Ormond, Vic., Australia). The image of the selected area was recorded on a black and white high-speed photographic film with the help of an attached camera assembly. Three representative images were recorded for each sample.

Statistical analysis

Each sample was analysed in triplicate. The digestion rate and extent of each starch were measured for the increase of the glucose concentration during the incubation at each designated time, and the values are expressed as means ± SE. Initial velocity of amylases hydrolysis of the starch was expressed as the slope of digestion curve within the first 1.5-h incubation time. Experimental data were subjected to the analysis of variance using GENSTAT 5 (Clarendon, NY, USA). Treatments were tested separately for least significant difference (LSD) at a 5% level of probability.

Results and discussion

Native starch morphology

The morphology of starch from the three wheat cultivars is shown in Fig. 1. All the three starches appeared to have both A-type and B-type granules (Fig. 1a–c), at which the starch displayed two sizes: large lenticular shaped granules (A-granules) and small spherical granules (B-granules) indicating their biosynthesis occurs at two different stages of the development (Fig. 1a–c). Starch from waxy wheat had a more spherical disc-like morphology compared with the two others, which was consistent with other reports (Kim & Huber, 2010). Moreover, further difference in the morphology of starches between waxy and normal wheat was also noticed, at that starch granules from normal wheat showed thicker than the starch from waxy wheat. These differences might be due to the formation of amylose molecules during biosynthesis. However, starch granules of high-amylose wheat display an irregular shape both for A-type and B-type granules (Fig. 1c). The visualisation in this study further confirmed that these starch granules are generally either small and spherical or large and ellipsoidal strongly depending on their botanical backgrounds. The irregular shapes of starch granules observed in this study for the high-amylose wheat further emphasises the importance of amylopectin as a parameter of granule morphogenesis during starch biosynthesis (Stinard *et al.*, 1993).

Starch morphology following cooking

The influence of cooking on starch morphology is displayed in Fig. 1a'–c'. In general, cooking led to the

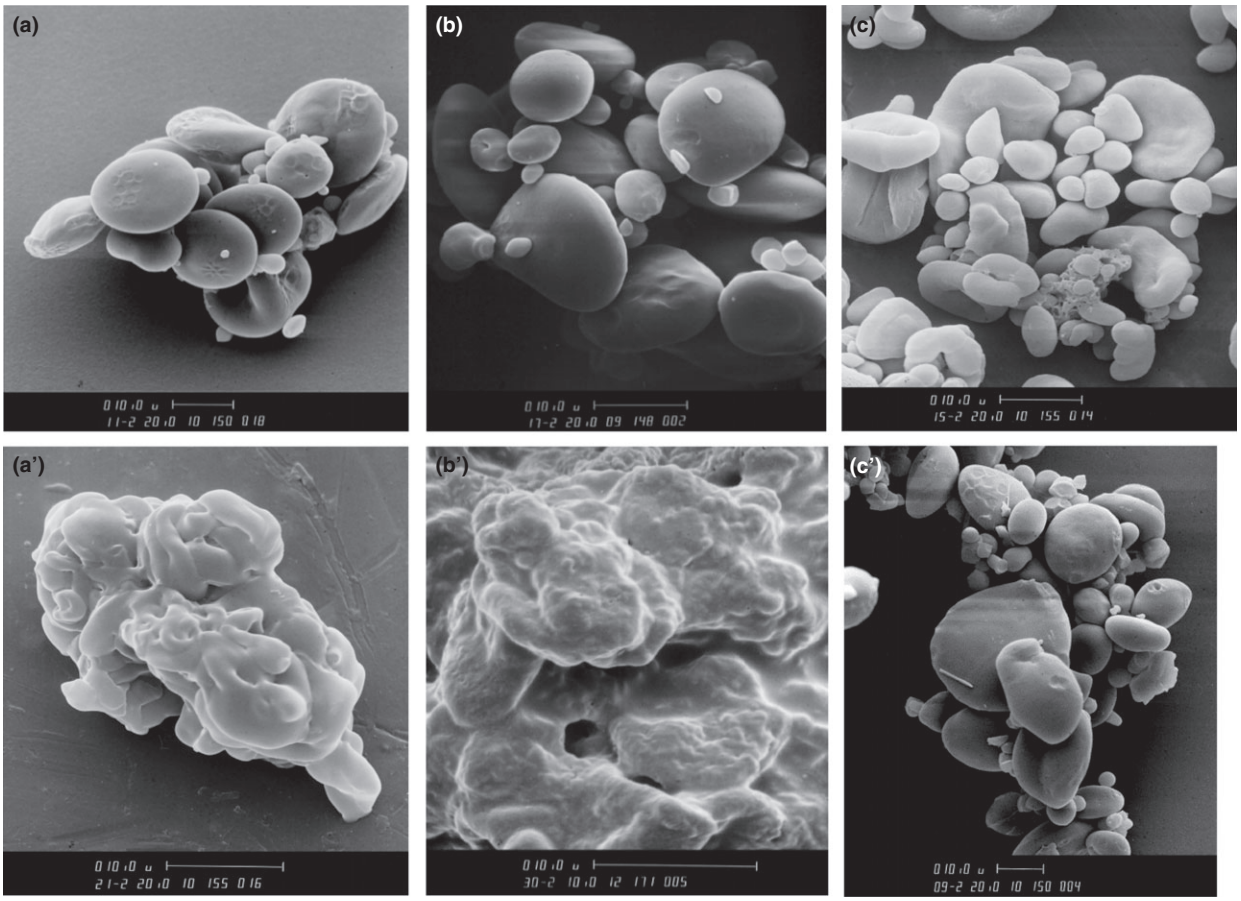

Figure 1 Morphology of starch granules following cook. a, a': native and cooked waxy wheat starch; b, b': native and cooked normal wheat starch; and c, c': native and cooked high-amylose wheat starch.

changes in their granule morphology. Starch granules from waxy and normal wheat were mostly gelatinised during the cooking, and they were adhesive together because of the leaching of starch molecules and thus demonstrated irregular shapes after the cooking. However, starch from the high-amylose wheat still had a granular shape at the end of cooking (Fig. 1c'), indicating its higher resistance to the cooking process.

Native starch morphology following digestion

The effect of digestion on starch morphology is presented in Fig. 2. It seems that amylase digestion starts from the surface pores and gradually enlarges the existing pores due to the internal corrosion by the enzymes for waxy and normal wheat starches (Fig. 2a and b). Following the further digestion process, the surface pores merged together forming larger channels/grooves resulting in hollow interiors ('inside out' digestion), and some intact granule fragments were observed alongside hollowed granules, probably arising from a minority of granules that have lower levels of pore. Crystalline blocklets are clearly evident in partly hydrolysed starch granules in the form of residues comprising small blocks that are tangentially arranged and tightly packed.

Although little is known on the preferably attacking spots of amylases on the surfaces of starch granules because of the lack of the understanding of the molecules distribution and their arrangement on the starch granule surface, this study at least displayed that the amylases digestion occurred on the lateral surface as well (Figure S1), suggesting the importance of molecular arrangement and the channels between the alternating zones of semicrystalline and amorphous regions in the granules.

The digestion of HAWS is presented in Fig 2c, which is characterised by a 'surface pitting' or an 'exo-corrosion', and 'surface scratching'. Meanwhile, the digestion of HAWS did not show the alternating zones of semicrystalline and amorphous as observed in the starch of waxy and normal wheat, indicating its

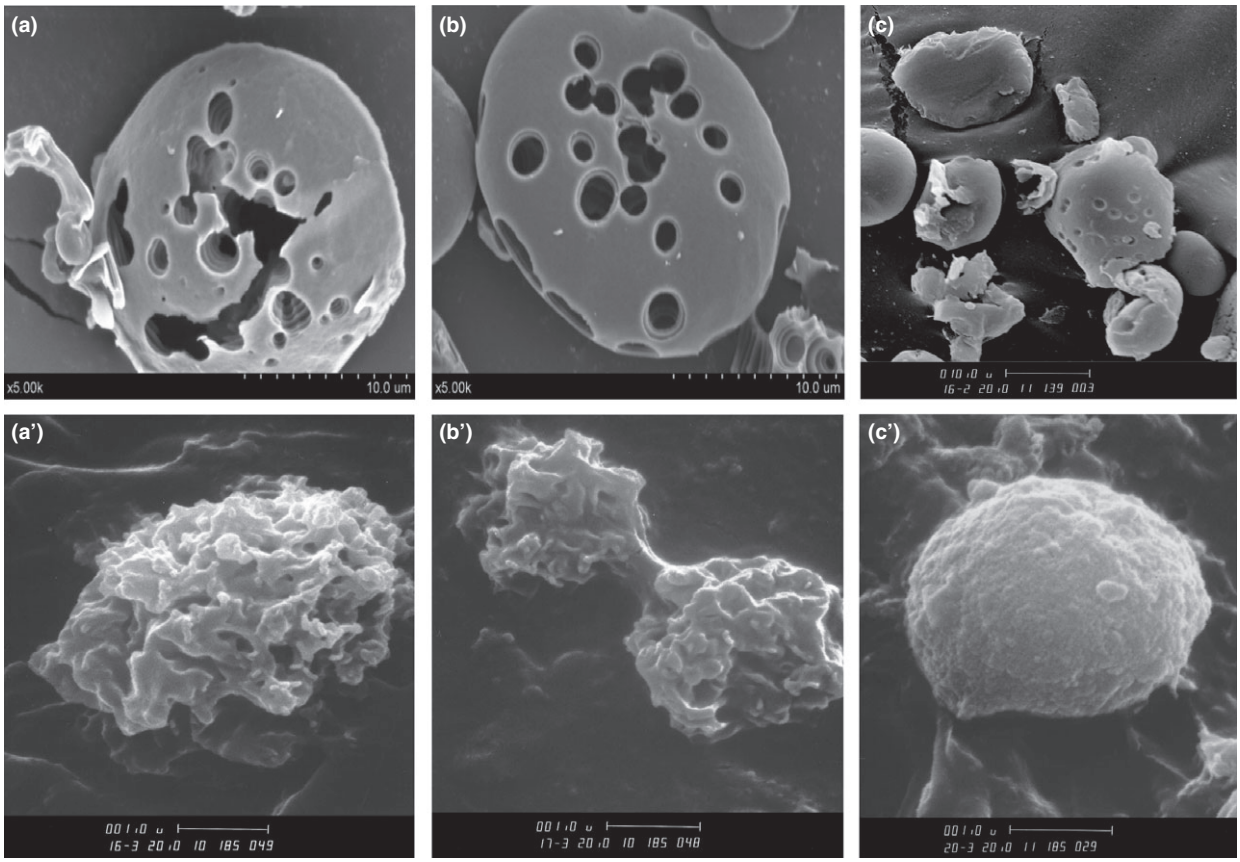

Figure 2 Starch morphology following digestion of 8 h. a, a': native and cooked waxy wheat starch; b, b': native and cooked normal wheat starch; and c, c': native and cooked high-amylose wheat starch.

different molecules arrangement in the granules. Particularly, this digestion character might be associated with its starch molecular arrangement on the surface layer of the starch granules.

Cooked starch morphology following digestion

The morphology of cooked waxy and normal wheat starch showed an alveolar shape or a faviform (Fig. 2a' and b'), which might indicate the digestion occurred on the particular regions in with a less organised structure. This digestion behaviour seems to be manipulated by the molecule distribution. The migration and rearrangement of the starch molecules during the gelatinisation and retrogradation process led to the redistribution of crystalline and amorphous regions in starch granules. Based on an assumption that amorphous regions penetrate through the entire granule and that on hydration they reversibly swell, forming a continuous gel, the removal of these amorphous regions by digestion would result in the morphology of starch particles with porosity structure (Fig. 2a' and b'). It is interesting to notice that digestion increased the evidence of the existence of the aggregate particles, which distribute on the surface of cooked HAWS (Fig. 2c'). It is assumed that aggregate particles form due to the rearrangement of starch molecules, and the low digestion rate and extent of HAWS are highly linked to the formation of these aggregates in starch.

Starch molecular structure by SE-HPLC

Chromatographic conditions for the separation of amylose and amylopectin molecules have been extensively studied previously (Shi *et al*., 1998; Pérez *et al*., 2013). The molecular features of the three starches under the current chromatographic conditions, illustrated in Fig. 3, showed that waxy wheat starch contained sole molecular fraction (Fra I) in its chromatograph. The MW measurement confirmed that it was amylopectin (7.11×10^7), indicating that there was exclusive amylose in its molecular profile. In normal wheat starch, two fractions (Fra I and Fra II) were eluted and represented as amylopectin and amylose, respectively, and

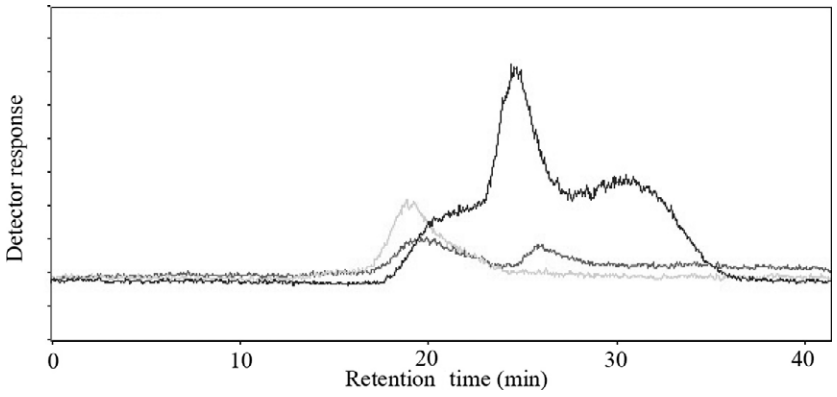

Figure 3 The molecular profile of wheat starch. Black line: high-amylose wheat; grey line: normal wheat; and light grey line: waxy wheat.

the amylose content was around 25% calculated from the ratio of two peaks in the profile. However, the starch molecules from the high-amylose wheat could be divided into three fractions on the basis of their MW: high MW fraction (Fra I, 3.97×10^7, mainly represented as amylopectin), medium MW fraction (Fra II, 4.19×10^5, amylose with relatively higher MW) and low MW fraction (Fra III, 9.23×10^3, amylose with relatively lower MW). Compared with the molecular features of the normal wheat starch, the molecular structure of HAWS was characterised by a higher proportion of lower MW amylose fraction. Similar to the molecular features of HAWS, the analysis of the molecular structure of maize starches with different amylose contents using a gel-permeation chromatography with refractive index detector and DMSO as mobile phase (Shi *et al.*, 1998) also showed that high-amylose maize starches (HYLON V and HYLON VII) contained two fractions of the amylose molecules, but not for normal maize starch.

Structural organisation by Fourier transform infra-red spectroscopy

The IR spectrum of the three wheat starches is presented in Figure S2 for attempting to interpret the variation in FTIR spectrum as a function of starch cultivars. In the IR range of 970–1035 cm^{-1}, the spectrum was characterised by the pattern of higher in left hand and lower in right hand for HAWS. However, the spectral pattern showed the otherwise for normal wheat starch. This difference in the absorbance intensity might be related to their corresponding molecular organisation in the starch granules. Bernazzani *et al.* (2001) and Zhou *et al.* (2010) suggest the band at 1022 cm^{-1} increases with the less organised structure of the starch, whereas the band at 1047 cm^{-1} (composed of two overlapping bands at 1040 and 1053 cm^{-1}) is related to the more organised structure of the starch. Thus, the overall starch structural organisation could be reflected by the ratio of 1047/1022 cm^{-1}, which represents the most characteristic of crystalline and amorphous regions in starch. This study showed that starch from high-amylose wheat had the highest IR ratio (0.68), followed by the starch from waxy wheat starch (0.55).

Starch molecules re-association by Fourier transform infra-red spectroscopy

Following the storage of the starch gel for 20 h, starch molecules are re-associated to form a new status. The re-association rate of starch molecules is monitored using a FTIR (Figure S3), and the changes in the IR ratio 1022/999–1047/1022 cm^{-1} are presented in Fig. 4 for differentiating their retrogradation process. Molecules from high-amylose starch showed the most quickly decrease in the IR ratio, indicating its molecules are more likely to re-associate with each other to

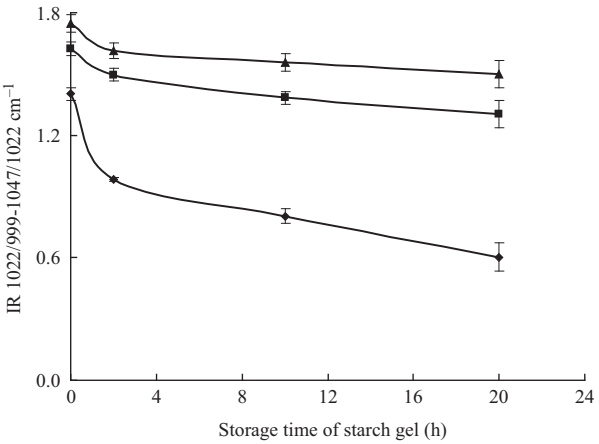

Figure 4 Changes in the IR ratio 1022/999–1047/1022 cm^{-1} following storage at 4 °C. ■:waxy wheat starch; ◆:normal wheat starch; and ▲: high-amylose wheat starch.

form a more organised structure than other starches. This study clearly shows that the retrogradation process is controlled by molecular characters (as studied in HPLC results section). In particular, the difference in amylose features between high-amylose wheat and normal wheat starch might be highly linked to the significant difference in their molecular characteristics ($P < 0.001$), and the existence of lower MW amylose fraction (Fra III) in the molecular profile of HAWS might play a key role for accelerating its retrogradation process.

Starch digestion kinetics

The digestion of the three native starches is divided into two stages: an initially rapid hydrolysis and a slower but more constant rate (Fig. 5). Starch from high-amylose wheat had a markedly slower digestion rate than the two others ($P < 0.001$). The understanding of the mechanism underlying this difference is of major significance in human nutrition, as normal and high-amylose starch granules have physiologically RS contents of <3% and more than 45%, respectively (Bird *et al*., 2009). Based on the current results, it might conclude that granule architecture features are the primary determinant of the large differences in enzyme susceptibility of different starch cultivars. As visualised by SEM, normal starch granules are readily expanded by enzyme digestion to provide a facile entry of enzymes to the less organised granule core for rapid digestion. Thus, the surface structure of these starch granules seems to be very important for controlling starch digestion at the first stage at which amylases could effectively pit the granule surface first and then penetrate through pinholes/internal channels and then hydrolyse the granule from inside-out. However, the visualisation of HAWS granules during the digestion does not show outstanding surface pores and so enzyme digestion has to proceed from the outside in, with the more molecularly organised outer layers of the granules providing a protecting barrier to the access of enzymes to the less organised granule interior. This observation is consistent with the limited literatures of mechanism studies on starch digestion (Evans & Thompson, 2004; Shrestha *et al*., 2012).

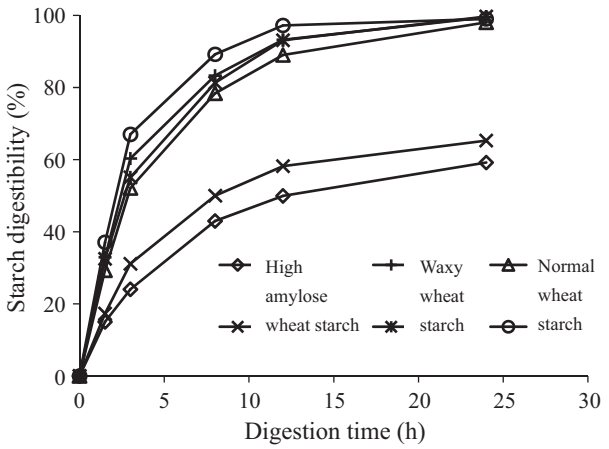

Figure 5 Digestion process of native and cooked wheat starch using a cocktail of enzymes. Each group indicates: upper symbol, cooked starch; bottom symbol: native starch.

Gelatinisation greatly enhances the chemical reactivity of inert starch granules towards amylolytic enzymes (Fig. 5). Starch granules swollen after the gelatinisation, which provided the more space for enzyme penetration, and the disruption of the organised array of starch molecules by cooking would enhance this situation. Cooking promoted the digestion rate and extent for all the starch substrates, but with different attitudes depending on the starch cultivars. Compared with its native form, cooking increased the digestion of waxy wheat starch at the greatest degree, followed by normal wheat starch. The digestion of HAWS led to a spherical morphology, and plenty of small aggregates were observed on its surface. The recent *in situ* study of starch gelatinisation and retrogradation under an ultra-high hydrostatic pressure using X-ray diffraction indicates that both waxy and high-amylose maize starches can be fully gelatinised at 5.9 and 5.1 GPa, respectively. However, in the case of waxy maize starch, upon release of pressure (to atmospheric pressure) crystalline structure appeared as a result of amylopectin aggregation, but not for high-amylose maize starch (Yang *et al*., 2013), which indicated that these two starches retrograded at different patterns. This study also implies that the crystalline parameter is not reliable for evaluating starch digestion properties (Shrestha *et al*., 2012). Most of the previous studies focused on the effect of amylose content on starch digestibility, and the relationship between the two parameters was observed in their experimental designs (Chung *et al*., 2010; Zhu *et al*., 2011). However, even more importantly, the recent study indicated that there were significant correlations between starch digestion rate and molecular structural characteristics, and the digestion rate tended to increase with longer amylose branches (Syahariza *et al*., 2013). Considering that the digestion of cooked HAWS follows a surface abrasion pattern (Fig. 2c'), it is assumed that the aggregates formed from amylose molecules, in particular low MW amylose during retrogradation process, would enhance structural organisation of starch granule surface, and thus manipulate its digestion properties.

Conclusions

Starch molecular structure manipulates starch morphology, cooking properties and its subsequent digestion

behaviours. This study found that amylases digestion occurred both on the superior surface and lateral surface, but it seems more preferable on the lateral one, indicating the importance of molecular arrangement on granule surface and the channels between the alternating zones of semicrystalline and amorphous regions in the granules. Three molecular fractions were detected in HAWS and characterised by a higher proportion of lower MW amylose fraction in its molecular profile. With such a molecular character, HAWS demonstrated the highest resistance to the amylases digestion among the three cultivars. Further analyses confirmed that starch containing high proportion of lower MW amylose fraction had a faster decrease in the IR ratio 1022/999–1047/1022 cm^{-1} during starch retrogradation process, indicating its molecules are more likely to re-associate with each other to form a more organised structure than other starch molecular features. Considering the unique properties of HAWS as revealed in this study, it might suggest that starch structure, in particular amylose structure, is more associated with resistance of starch to the enzyme digestion rather than amylose content alone.

Acknowledgment

This work is funded by Science and Technology Department, China, through a China–European research collaboration programme (Grant: SQ2013ZO A100-001).

References

AACC International. (2000). *Approved Methods of the AACC International* (9th edn). Methods 61-03. St. Paul, MN: American Association of Cereal Chemists.

Barcelo, A., Claustre, J., Moro, F., Chayvialle, J.A., Cuber, J.C. & Plaisancie, P. (2000). Mucin secretion is modulated by luminal factors in the isolated vascularly perfused rat colon. *Gut*, **46**, 218–224.

Bernazzani, P., Chapados, C. & Delmas, G. (2001). Phase change in amylose–water mixtures as seen by Fourier transform infrared. *Biopolymers*, **58**, 3305–3318.

Bird, A.R., Brown, I.L. & Topping, D.L. (2000). Starches, resistant starches, the gut microflora and human health. *Current Issues in Intestinal Microbiology*, **1**, 25–37.

Bird, A.R., Vuaran, M.S., King, R.A. *et al.* (2008). Wholegrain foods made from a novel high-amylose barley variety (Himalaya 292) improve indices of bowel health in human subjects. *British Journal of Nutrition*, **99**, 1032–1040.

Bird, A.R., Lopez-Rubio, A., Shrestha, A.K. & Gidley, M.J. (2009). Resistant starch in vitro and in vivo: factors determining yield, structure, and physiological relevance. In: *Modern Biopolymer Sciences* (edited by S. Kasapis, I.T. Norton & J.B. Ubbink). Pp. 449–510. London: Academic Press Inc.

Björck, I.M., Granfeldt, Y., Liljeberg, H., Tovar, J. & Asp, N.G. (1994). Food properties affecting the digestion and absorption of carbohydrates. *The American Journal of Clinical Nutrition*, **59**, 699S–705S.

Chung, H.J., Liu, Q.A., Wang, R.L., Yin, Y.L. & Li, A.K. (2010). Physicochemical properties and in vitro starch digestibility of cooked rice from commercially available cultivars in Canada. *Cereal Chemistry*, **87**, 297–304.

Englyst, H.N. & Hudson, G.J. (1996). The classification and measurement of dietary carbohydrates. *Food Chemistry*, **57**, 15–21.

Englyst, H.N., Kingman, S.M. & Cummings, J.H. (1992). Classification and measurement of nutritionally important starch fractions. *European Journal of Clinical Nutrition*, **46**, S33–S50.

Evans, A. & Thompson, D.B. (2004). Resistance to alpha-amylase digestion in four native high-amylose maize starches. *Cereal Chemistry*, **81**, 31–37.

Finnie, S.M., Jeannotte, R., Morris, C.F., Giroux, M.J. & Faubion, J.M. (2010). Variation in polar lipids located on the surface of wheat starch. *Journal of Cereal Science*, **51**, 73–80.

Frei, M., Siddhuraju, P. & Becker, K. (2003). Studies on the in vitro starch digestibility and the glycemic index of six different indigenous rice cultivars from the Philippines. *Food Chemistry*, **83**, 395–402.

Htoon, A., Shrestha, A.K., Flanagan, B.M., Lopez-Rubio, A., Bird, A.R. & Gilbert, E.P. (2009). Effects of processing high amylose maize starches under controlled conditions on structural organization and amylase digestibility. *Carbohydrate Polymers*, **75**, 236–245.

Kim, H.S. & Huber, K.C. (2010). Physicochemical properties and amylopectin fine structures of A- and B-type granules of waxy and normal soft wheat starch. *Journal of Cereal Science*, **51**, 256–264.

Kumar, S. & Prabhasankar, P. (2014). Low glycemic index ingredients and modified starches in wheat based food processing: a review. *Trends in Food Science and Technology*, **35**, 32–41.

Ludwig, D.S. (2003). Glycemic load comes of age. *The Journal of Nutrition*, **133**, 2695–2696.

Man, J., Yang, Y., Zhang, C. *et al.* (2012). Structural changes of high-amylose rice starch residues following in vitro and in vivo digestion. *Journal of Agricultural and Food Chemistry*, **60**, 9332–9341.

Pérez, E., Rolland-Sabaté, A., Dufour, D. *et al.* (2013). Isolated starches from yams (Dioscorea sp.) grown at the Venezuelan Amazons: structure and functional properties. *Carbohydrate Polymers*, **98**, 650–658.

Regina, A., Bird, A., Topping, D. *et al.* (2006). High amylose wheat generated by RNA interference improves indices of large bowel health in rats. *Proceedings of the National Academy of Science of the United States of America*, **103**, 3546–3551.

Shi, Y.C., Capitani, T., Trzasko, P. & Jeffcoat, R. (1998). Molecular structure of a low-amylopectin starch and other high-amylose maize starches. *Journal of Cereal Science*, **27**, 289–299.

Shrestha, A.K., Blazek, J., Flanagan, B.M. *et al.* (2012). Molecular, mesoscopic and microscopic structure evolution during amylase digestion of maize starch granules. *Carbohydrate Polymers*, **90**, 23–33.

Skrabanja, V., Liljeberg, H.G.M., Hedley, C.L., Kreft, I. & Björck, I.M.E. (1999). Influence of genotype and processing on the in vitro rate of starch hydrolysis and resistant starch hydrolysis in peas (*Pisumsativum* L.). *Journal of Agricultural and Food Chemistry*, **47**, 2033–2039.

Slaughter, S.L., Ellis, P.R. & Butterworth, P.J. (2001). An investigation of the action of porcine pancreatic α-amylase on native and gelatinised starches. *Biochimica et Biophysica Acta*, **1525**, 29–36.

Stinard, P.S., Robertson, D.S. & Schnable, P.S. (1993). Genetic isolation, cloning, and analysis of a mutator-induced, dominant antimorph of the maize amylose extender1 Locus. *Plant Cell*, **5**, 1555–1566.

Świeca, M., Baraniak, B. & Gawlik-Dziki, U. (2013). In vitro digestibility and starch content, predicted glycemic index and potential in vitro antidiabetic effect of lentil sprouts obtained by different germination techniques. *Food Chemistry*, **138**, 1414–1420.

Syahariza, Z.A., Sar, S., Hasjim, J., Tizzotti, M.J. & Gilbert, R.G. (2013). The importance of amylose and amylopectin fine structures for starch digestibility in cooked rice grains. *Food Chemistry*, **136**, 742–749.

Topping, D.L. & Clifton, P.M. (2001). Short-chain fatty acids and human colonic function: roles of resistant starch and nonstarch polysaccharides. *Physiological Reviews*, **81**, 1031–1064.
Tovar, J., Björck, I.M. & Asp, N.G. (1992). Incomplete digestion of legume starches in rats: a study of precooked flours containing retrograded and physically inaccessible starch fractions. *The Journal of Nutrition*, **122**, 1500–1507.
Yang, Z., Gu, Q. & Hemar, Y. (2013). *In situ* study of maize starch gelatinization under ultra-high hydrostatic pressure using X-ray diffraction. *Carbohydrate Polymers*, **97**, 235–238.
Zhou, Z.K., Topping, D., Morell, M. & Bird, A. (2010). Changes in starch physical characteristics following digestion of foods in the human small intestine. *British Journal of Nutrition*, **104**, 573–581.
Zhou, Z.K., Zhang, Y., Zheng, P.Y. & Chen, X.S. (2013). Starch structure modulates metabolic activity and gut microbiota profile. *Anaerobe*, **24**, 71–78.
Zhu, L.J., Liu, Q.Q., Wilson, J.D., Gu, M.H. & Shi, Y.C. (2011). Digestibility and physicochemical properties of rice (*Oryza sativa* L.) flours and starches differing in amylose content. *Carbohydrate Polymers*, **86**, 1751–1759.

Supporting Information

Additional Supporting Information may be found in the online version of this article:

Figure S1. The morphology of starch granules following digestion.

Figure S2. The IR spectrum of three native wheat starches.

Figure S3. The IR spectrum of wheat starch gel following storage at 4 °C for 20 h.